Surface resonant states and superlensing in acoustic metamaterials

Muralidhar Ambati, Nicholas Fang, Cheng Sun, and Xiang Zhang*
Center for Scalable and Integrated Nanomanufacturing (SINAM), University of California, Berkeley, California 94720, USA
(Received 19 April 2007; published 31 May 2007)

We report that the negative material responses of acoustic metamaterials can lead to a plethora of surface resonant states. We determine that negative effective-mass density is the necessary condition for the existence of surface states on acoustic metamaterials. We offer the microscopic picture of these unique surface states; in addition, we find that these surface excitations enhance the transmission of evanescent pressure fields across the metamaterial. The evanescent pressure fields scattered from an object can be resonantly coupled and enhanced at the surface of the acoustic metamaterial, resulting in an image with resolution below the diffraction limit. This concept of acoustic superlens opens exciting opportunities to design acoustic metamaterials for ultrasonic imaging.

DOI: 10.1103/PhysRevB.75.195447 PACS number(s): 43.20.+g, 43.35.+d, 46.40.Ff

I. INTRODUCTION

Advances in electromagnetic metamaterials[1,2] offer excellent opportunities to realize new and exotic phenomena, such as negative refraction[3] and artificial magnetism.[4,5] Its acoustic counterpart with negative material properties has been recently explored.[6–9] Acoustic metamaterials with locally resonant elements can be designed to display anomalous response at selected frequencies so that effective dynamic material properties can be negative. It should be noted that the effective negative properties of the metamaterials are dynamic and highly dispersive. Such acoustic metamaterials offer a possible route to the realization of intriguing phenomena; negative refraction was reported earlier in double negative acoustic metamaterials.[8]

Recent work on phononic crystals—periodic modulation of density and modulus—also showed that negative refraction and focusing of acoustic waves[10–12] can be obtained from band-folding effects due to Bragg scattering. Phononic crystals require that the spatial modulation of impedance is of the same order as the acoustic wavelength.[13–19] Metamaterials provide a major step toward an effective-medium description, as the spatial periodic modulation of impedance is much smaller than the wavelength. Acoustic metamaterials, also referred as sonic crystals, have been considered as spectral gap materials[6,20–22] and refractory acoustic devices.[23,24] Metamaterials broaden the range of material responses found in nature, which can be especially useful in realizing new phenomena and in designing novel devices. Yet to the best of our knowledge, there has been very limited investigation in this direction. In this paper, we report a surface resonance on an acoustic metamaterial and examine its unique characteristics. As a result of this surface resonance, we propose and numerically demonstrate an acoustic superlens—analogous to Pendry's perfect lens[25]—for sub-diffraction-limited acoustic imaging.

II. SURFACE STATES ON AN ACOUSTIC METAMATERIAL

We consider a plane harmonic longitudinal wave analysis at a boundary between a fluid half-space and an acoustic metamaterial half-space [Fig. 1(a)]. Medium I is considered as a fluid, with positive mass density and bulk modulus, whereas medium II is taken as an acoustic metamaterial. In a homogeneous medium with mass density ρ and bulk modulus B, the equilibrium equation and mass continuity equation are written in the index notation to relate the pressure P and velocity field v_i at any given point,

$$k_i P - \rho\omega v_i = 0, \quad k_i v_i - \omega\frac{P}{B} = 0, \tag{1}$$

where k_i and ω are the wave vector and angular frequency of the plane wave.

Let us consider the necessary and sufficient conditions that allow the existence of surface states at the interface between a fluid and an acoustic metamaterial, the latter being modeled as a structured isotropic fluid. Structured fluid consists of the same fluid as medium I as the matrix with acoustic resonators in it. The surface states represent elastic perturbations with pressure—maximum at the interface and exponentially decaying in the direction perpendicular to the interface—schematically shown in Fig. 1(a). By matching pressure and normal velocity fields at the interface ($z=0$), we obtain the relation between the normal components of wave vectors:

$$\frac{k_z^{\mathrm{I}}}{\rho^{\mathrm{I}}} + \frac{k_z^{\mathrm{II}}}{\rho^{\mathrm{II}}} = 0. \tag{2}$$

The necessary condition for a bound state to exist at the interface requires that both k_z's have positive imaginary parts, which implies that the mass density of the acoustic metamaterial should be negative ($\rho^{\mathrm{II}}<0$). Negative density implies that the response of fluid—acceleration—is out of phase with the dynamic pressure gradient, and it is obtained when such negative responses of the oscillators constituting the acoustic metamaterial dominate the background. The dynamic effective-mass density of the metamaterials can be significantly different from the volume averaged mass density,[26,27] as the multiple scattering is treated in an average sense.[26] Negative effective-mass density is reported for fluid-solid composites, e.g., soft rubber spheres in water.[8] In general, acoustic metamaterial can be modeled as a set of har-

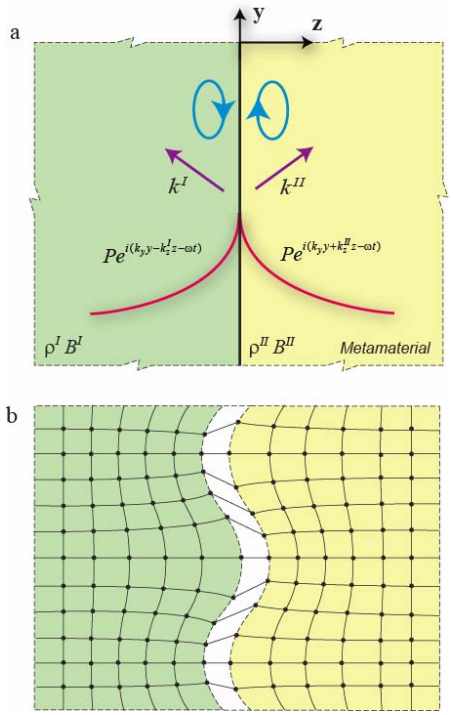

FIG. 1. (Color online). Schematic of the surface state at an interface separating two semi-infinite media. Medium I is considered to have positive material properties (mass density ρ and bulk modulus B), whereas medium II is taken as an acoustic metamaterial with generic material properties. All the physical quantities pertaining to the medium are designated by the respective medium superscript. (a) Schematic of the pressure profile of surface bound states; it is maximum at the interface and decaying exponentially perpendicular to the interface. The motion trajectory of the material points is an ellipse; the elliptical rotation of the particles near the interface is the same in both media (shown clockwise). The eccentricity of the ellipses depends on the wave vector of the surface state with major axes parallel to the interface. (b) The pattern of the displacements of the surface wave is illustrated (top view). The schematic shows that the displacements in y and z directions are 90° out of phase, with slipping at the interface.

monic oscillators. Here, surface resonance corresponds to the oscillation of harmonic oscillators such that there is constant slipping at the interface. Given effective negative mass density, the slip arises due to the difference in tangential velocities that changes the direction across the interface. By calculating the components of the velocities along the y and z axes by Eq. (1), we obtain that the velocity components are shifted in phase by $\pi/2$. Therefore, the trajectories of the particle motions are ellipses with major axes parallel to the interface, and the elliptical rotation of the particles near the interface remains the same in both the media [Fig. 1(a)]. In contrast to this surface state, the particle trajectories in the Rayleigh wave are elliptical with major axis perpendicular to the interface and the rotation changing with depth. In addition, the pattern of the displacements in the unique surface state is illustrated [Fig. 1(b)].

III. DISPERSION RELATION OF THE SURFACE STATES

We derive the surface-state dispersion between the angular frequency ω of the surface states and the wave vector k_y by combining Eq. (2) with the dispersion relations of media I and II, $(k_y^2)^{\mathrm{I,II}}+(k_z^2)^{\mathrm{I,II}}=\omega^2(\rho/B)^{\mathrm{I,II}}$, The tangential wave vector k_y is required to be continuous across the interface, resulting in the dispersion relation of surface states,

$$k_y^2 = \omega^2 \frac{\rho^{\mathrm{I}}\rho^{\mathrm{II}}}{(\rho^{\mathrm{II}})^2 - (\rho^{\mathrm{I}})^2}\left(\frac{\rho^{\mathrm{II}}}{B^{\mathrm{I}}} - \frac{\rho^{\mathrm{I}}}{B^{\mathrm{II}}}\right). \tag{3}$$

In addition to the necessary condition ($\rho^{\mathrm{II}}<0$), surface bound states require that $k_y^2 > k_0^2 = \omega^2(\rho^{\mathrm{I}}/B^{\mathrm{I}})$. This inequality and Eq. (3) are used to determine the conditions on the properties of acoustic metamaterial that support the surface states. In the case $|\rho^{\mathrm{II}}|>\rho^{\mathrm{I}}$, the bulk modulus of the acoustic metamaterial should be either positive, $B^{\mathrm{II}}>0$, or negative satisfying the inequality $B^{\mathrm{II}}<\rho^{\mathrm{II}}B^{\mathrm{I}}/\rho^{\mathrm{I}}$. On the other hand, for the case $|\rho^{\mathrm{II}}|<\rho^{\mathrm{I}}$, the bulk modulus of the acoustic metamaterial should be negative and $B^{\mathrm{II}}>\rho^{\mathrm{II}}B^{\mathrm{I}}/\rho^{\mathrm{I}}$.

We find that when the bulk moduli of two media are the same (B), the dispersion relation of surface states reduces to

$$k_y^2 = \frac{\omega^2}{B}\left(\frac{\rho^{\mathrm{I}}\rho^{\mathrm{II}}}{\rho^{\mathrm{I}} + \rho^{\mathrm{II}}}\right). \tag{4}$$

Similar to the surface-plasmon resonance in electromagnetics, negative mass density in acoustic metamaterials significantly broadens the surface resonant band of k_y in the limit of $\rho^{\mathrm{II}}(\omega)\rightarrow(-\rho^{\mathrm{I}})$. This broadening is represented by the flat dispersion curve that is wave vector independent (Fig. 2). The bulk modulus of both the media is taken to be the same, $B^{\mathrm{II}}=B^{\mathrm{I}}$. The effective-mass density of medium II—a structured fluid—is taken in Lorentz form.[7] Linear-response functions such as mass density take the Lorentz form $1/(\omega_o^2 - \omega^2)$, in the case where a wave of angular frequency ω interacts with a medium consisting of localized resonator with resonant frequency ω_o.[6] Here, we consider only the frequency interval in which the surface state exists: effective-mass density of medium II is negative and greater in magnitude than medium I, $\rho^{\mathrm{II}}(\omega)<0$ and $|\rho^{\mathrm{II}}(\omega)|>\rho^{\mathrm{I}}$. Dispersion curve for the surface resonance is shown in red, and the linear dispersion curve of medium I is shown in blue. It is evident that the wave vector of the surface wave is always greater than that of the bulk wave in medium I.

IV. CHARACTERISTICS OF THE SURFACE STATES

We consider a thin slab of acoustic metamaterial whose effective-mass density is negative in the near field of an object. We find that the evanescent pressure fields, scattered from the object, can be resonantly coupled onto the surface states and transmitted through the slab with enhanced amplitude. Evanescent pressure fields are in which the pressure and velocity fluctuations are shifted in phase by $\pi/2$, and they exist in near field decaying exponentially away from the object. Transmission enhancement is due to the bound states on the surface acting as an energy reservoir, wherein the surface states take energy from the source and enhance the

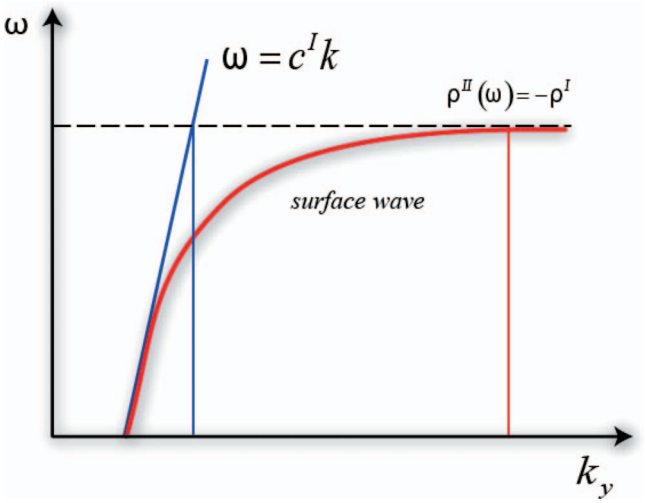

FIG. 2. (Color online) Dispersion curve of the surface state at the interface between two semi-infinite media with mass densities of opposite signs. The effective-mass density of the medium II—an acoustic metamaterial—is taken in Lorentz form, and the frequency interval is considered in which the surface states exist, $\rho^{\mathrm{II}}(\omega)<0$ and $|\rho^{\mathrm{II}}(\omega)|>\rho^{\mathrm{I}}$. The bulk modulus of both media is taken to be same, $B^{\mathrm{II}}=B^{\mathrm{I}}$. Dispersion curve for the surface resonance is shown in, and it is clear that in the limit of $\rho^{\mathrm{II}}(\omega)\to-\rho^{\mathrm{I}}$, the dispersion curve asymptotically reaches infinity. Also, the linear dispersion curve of medium I is shown in blue. The vertical lines in the figure depict the x intercepts (wave vectors at a given frequency), and it is clear that the wave vector of the surface wave is always greater than that of the bulk wave in medium I.

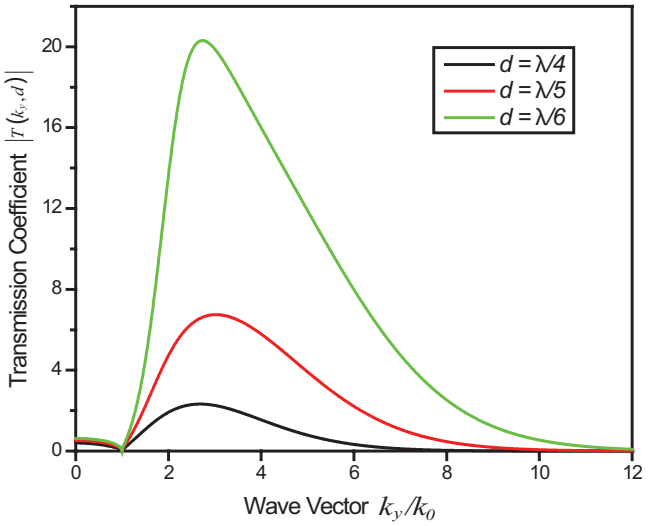

FIG. 3. (Color online). Enhanced transmission of evanescent pressure waves across an acoustic metamaterial, a slab of negative effective-mass density. Different thicknesses (d) of the acoustic metamaterials are considered, and in each case the effective-mass density of the acoustic metamaterial is taken as $\rho^{\mathrm{II}}=(-1+0.01i)\rho^{\mathrm{I}}$. The bulk modulus is assumed to be same as that of the surrounding medium, $B^{\mathrm{II}}=B^{\mathrm{I}}$. $|T(k_y,d)|$ is the ratio of amplitude of pressure fields across the metamaterial. Enhanced transmittivity—the wave-vector range over which the evanescent waves are transmitted with increased amplitude—is a strong function of the thickness of the slab (d), as the thickness determines the coupling of surface states at the two interfaces.

amplitude of evanescent waves. The degree of enhancement across a finite slab of acoustic metamaterial depends on the thickness of acoustic metamaterial, which, in turn, determines the resonant coupling of surface states at the two interfaces.

Given an acoustic metamaterial II of finite thickness d placed in a medium I, the overall transmission coefficient T—ratio of pressure fields—across the acoustic metamaterial can be computed by taking account of multiple scattering events similar to the electromagnetic case.[25]

$$T(k_y,d)=\frac{tt'\exp(ik_z^{\mathrm{II}}d)}{1+rr'\exp(i2k_z^{\mathrm{II}}d)}, \tag{5}$$

where

$$r=\frac{\frac{k_z^{\mathrm{I}}}{\rho^{\mathrm{I}}}-\frac{k_z^{\mathrm{II}}}{\rho^{\mathrm{II}}}}{\frac{k_z^{\mathrm{I}}}{\rho^{\mathrm{I}}}+\frac{k_z^{\mathrm{II}}}{\rho^{\mathrm{II}}}}, \quad r'=-r, \quad t=1+r, \quad t'=1+r'.$$

t and t' are the pressure transmission coefficients at the interface of I/II and II/I, respectively. Similarly, r and r' are the corresponding pressure reflection coefficients. The exponential growth of overall transmission for evanescent pressure fields is valid when $|rr'|\gg 1$. This inequality implies a diverging reflectivity on either surface, that is, $k_z^{\mathrm{I}}/\rho^{\mathrm{I}}+k_z^{\mathrm{II}}/\rho^{\mathrm{II}}\to 0$, which is exactly the condition we obtain for surface resonance in Eq. (2). Figure 3 displays the overall transmission of a wide range of wave vectors across the acoustic metamaterial of different thicknesses. It clearly demonstrates the enhancement of evanescent waves ($k_y/k_0>1$), a key feature of the surface resonance. However, there is no exponential growth in the case of nonzero losses. In these calculations, we consider acoustic metamaterial—medium II—to have complex effective-mass density with negative real part and positive imaginary part.[7] The positive imaginary part of effective-mass density corresponds to the loss in the metamaterial, which is a dynamic average of various microscopic relaxation phenomena—leading to bulk viscosity—in the constituent materials of the metamaterial. The demonstrated enhancement of evanescent waves in acoustic metamaterial (Fig. 3) gives rise to the possibility of restoring the amplitude of the wide range of evanescent components, and thus leading to sub-diffraction-limited imaging, i.e., superlensing.

V. ACOUSTIC SUPERLENS

We propose a perfect acoustic lens analogous to Pendry's perfect lens[25] in two different ways. The first prospect is an acoustic metamaterial whose effective material properties—mass density and bulk modulus—are simultaneously negative and perfectly matched, impedancewise, to the surrounding medium. The second one is an acoustic metamaterial that has negative mass density and positive bulk modulus—which are equal in magnitude to those of the surrounding medium—with thickness smaller than the acoustic wave-

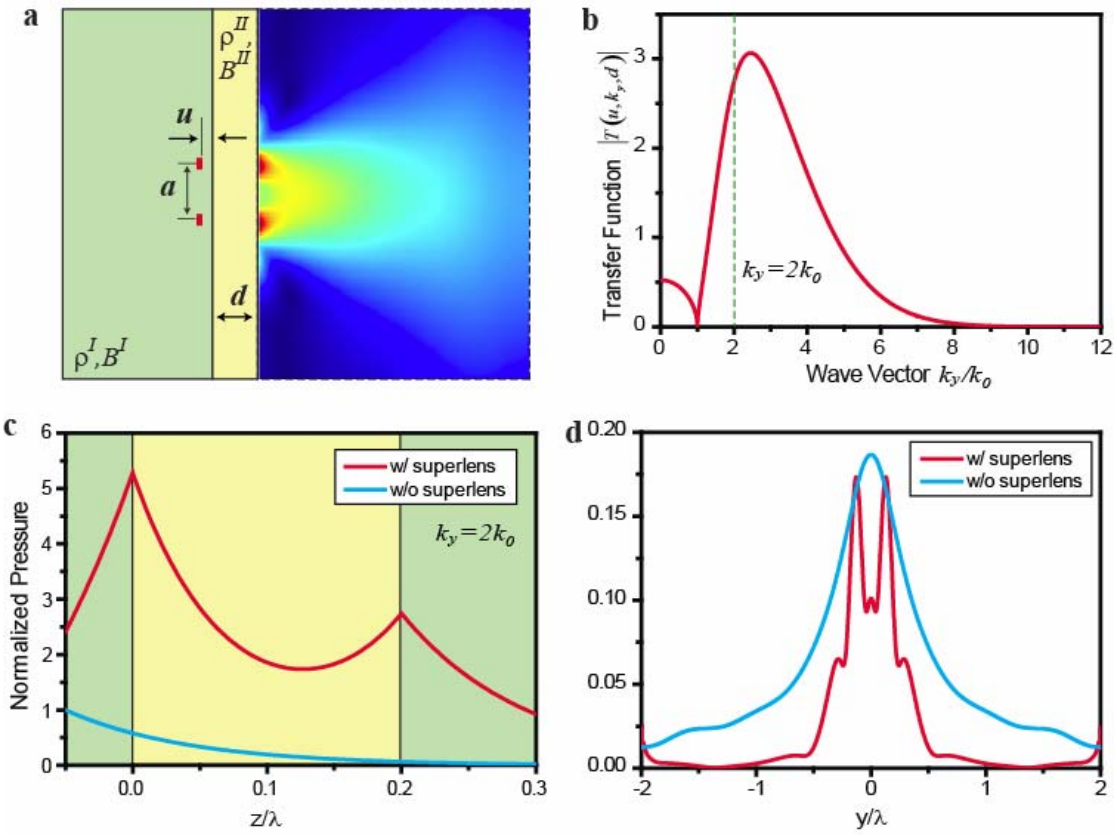

FIG. 4. (Color online) Acoustic superlensing with a slab of effective negative mass density. (a) The configuration considered is as follows: $a=\lambda/4$, $d=\lambda/5$, $u=\lambda/20$, and $\rho^{II}=(-1+0.01i)\rho^{I}$. A slab of negative mass density of thickness d is placed in medium I. Two sources separated by a are placed at a distance u from the slab. The pressure field (amplitude) distribution after finite element analysis shown at the right resolves the two sources. (b) The transfer function—the modulus of image pressure field normalized by object pressure field in wave-vector space—shows that the evanescent waves in the interval $[1.3k_0, 4.8k_0]$ are enhanced. Image plane is taken at the interface separating media II and I. (c) The amplitude of evanescent pressure field ($k_y=2k_0$) normalized to the amplitude in object plane clearly shows the enhancement with local maximum at each of the interfaces (red). The blue line is the control without the superlens, which shows an exponential decay of the amplitude of the evanescent pressure field. The abscissa is the z coordinate normalized to the wavelength. (d) The pressure field amplitude in the image plane with (red) and without (blue) the acoustic superlens. The presence of acoustic superlens offers enough contrast to resolve the object.

length. We find that in the quasistatic limit, the dependence on modulus is eliminated and only mass densities are relevant for pressure fields. We consider such an acoustic metamaterial slab with effective negative mass density as a superlens in acoustics, which offers highly localized surface acoustic waves over a broad evanescent wave-vector spectrum. However, the loss in the acoustic metamaterial and the unit-cell dimensions of metamaterial impose practical limitations on imaging resolution. The loss in acoustic metamaterial depends on the structure of metamaterial, the losses in the constituent materials of metamaterial, and the frequency of operation. In addition to the loss in acoustic metamaterial, the unit-cell dimensions of the acoustic metamaterial (a) affects the resolution. This limitation occurs as the evanescent waves of large lateral wave vector k_y interact with the inhomogeneity of the acoustic metamaterials, and the average over the metamaterial—effective medium description—does not hold for evanescent waves whose k_y is comparable to $2\pi/a$.

We use numerical simulations to demonstrate the acoustic superlens effect with a thin slab of lossy homogenized material of positive bulk modulus and negative mass density. The wave equation, $\nabla\cdot-[(1/\rho)\nabla P]-\omega^2(P/\rho c^2)=0$, is solved in computational domain displayed in Fig. 4(a) using FEMLAB,[28] where c is the speed of acoustic wave. Two sources width $\lambda/20$, separated by a distance of $\lambda/4$, emanating from waveguides are taken as the object. The boundary conditions are as follows: the walls of the waveguides are rigid and pressure waves are only interacting with the surrounding medium at the exit. In addition, the boundaries of the computational domain are taken as nonreflecting. Pressure field distribution in the presence of the slab of negative mass density, thickness $\lambda/5$, is plotted in Fig. 4(a). It is clearly evident that the presence of the slab offers enough contrast to resolve the two sources. Since the image is primarily formed by evanescent waves, there is no fixed focal plane. The best contrast is at the interface between media II and I; therefore, it is considered as the image plane. The resolving power of the slab—acting as an acoustic superlens—is obtained from the transfer function, ratio of the image pressure fields to object pressure fields. It is calculated from Eq. (5), accounting for the additional decay from the

object to the lens. Figure 4(b) illustrates that a range of evanescent waves in the interval $[1.3k_0, 4.8k_0]$ can be enhanced and recovered in the image plane. Figure 4(c) shows the enhancement of an evanescent pressure wave ($k_y = 2k_0$) coupled to the surface bound states. Calculations show that there is a local maximum on the surfaces of the slab and a net enhancement from the object plane to the image plane. In Fig. 4(d), we plot the pressure amplitude distribution in the image plane—transfer function $|T(u, k_y, d)|$ convoluted with object wave-vector spectrum—with and without the slab of negative mass density. Negative mass density slab offers high contrast at the image plane by enhancing the evanescent pressure fields—that carry finer details of the object—and at the same time damping the propagating pressure fields. It is numerically demonstrated that a flat slab of negative mass density can be used as an acoustic lens for subwavelength imaging. Such a slab of material acts as a superlens which can overcome the limitation of traditional lens performance. In contrast to the superlens discussed, there exists a mode where the Lamb waves—coupled Rayleigh surface waves—are highly localized.[29] The coupled wave-vector spectrum with Lamb waves at this frequency provides an improved signal-to-noise ratio but does not overlap with evanescent wave-vector spectrum, and hence there is no superresolution.

VI. CONCLUSIONS

In conclusion, we propose a different surface resonance phenomenon in acoustics. Unlike in electromagnetics, where negative permittivity and permeability control *P* and *S* polarized surface states, respectively, it is proved here that only negative mass density is necessary for the surface resonance in acoustics. These surface resonant states and superlensing are likely to stimulate research in the design of acoustic metamaterials and devices.

ACKNOWLEDGMENTS

Financial support from the ONR (Grant No. N000140710626) and ONR/DARPA Multidisciplinary University Research Initiative (MURI) (Grant No. N00014-01-1-0803) is acknowledged. The authors also acknowledge helpful discussions with J. Sau and D. K. Gramotnev.

*Author to whom correspondence should be addressed. Email address: xiang@berkeley.edu

[1] D. R. Smith, J. B. Pendry, and M. C. K. Wiltshire, Science **305**, 788 (2004).
[2] J. B. Pendry, A. J. Holden, W. J. Stewart, and I. Youngs, Phys. Rev. Lett. **76**, 4773 (1996).
[3] R. A. Shelby, D. R. Smith, and S. Schultz, Science **292**, 77 (2001).
[4] J. B. Pendry, A. J. Holden, D. J. Robbins, and W. J. Stewart, IEEE Trans. Microwave Theory Tech. **47**, 2075 (1999).
[5] S. Linden, C. Enkrich, M. Wegener, J. Zhou, T. Koschny, and C. M. Soukoulis, Science **306**, 1351 (2004).
[6] Z. Liu, X. Zhang, Y. Mao, Y. Y. Zhu, Z. Yang, C. T. Chan, and P. Sheng, Science **289**, 1734 (2000).
[7] Z. Liu, C. T. Chan, and P. Sheng, Phys. Rev. B **71**, 014103 (2005).
[8] J. Li and C. T. Chan, Phys. Rev. E **70**, 055602(R) (2004).
[9] N. Fang, D. Xi, J. Xu, M. Ambati, W. Srituravanich, C. Sun, and X. Zhang, Nat. Mater. **5**, 452 (2006).
[10] X. D. Zhang and Z. Liu, Appl. Phys. Lett. **85**, 341 (2004).
[11] S. X. Yang, J. H. Page, Z. Liu, M. L. Cowan, C. T. Chan, and P. Sheng, Phys. Rev. Lett. **93**, 024301 (2004).
[12] M. Torres and F. R. Montero de Espinosa, Ultrasonics **42**, 787 (2004).
[13] M. M. Sigalas and E. N. Economou, J. Sound Vib. **158**, 377 (1992).
[14] M. S. Kushwaha, P. Halevi, L. Dobrzynski, and B. Djafari-Rouhani, Phys. Rev. Lett.. **71**, 2022 (1993).
[15] M. Kafesaki and E. N. Economou, Phys. Rev. B **52**, 13317 (1995).
[16] F. R. Montero de Espinosa, E. Jiménez, and M. Torres, Phys. Rev. Lett. **80**, 1208 (1998).
[17] I. E. Psarobas, N. Stefanou, and A. Modinos, Phys. Rev. B **62**, 5536 (2000).
[18] J. O. Vasseur, P. A. Deymier, B. Chenni, B. Djafari-Rouhani, L. Dobrzynski, and D. Prevost, Phys. Rev. Lett. **86**, 3012 (2001).
[19] T. T. Wu, Z. G. Huang, and S. Lin, Phys. Rev. B **69**, 094301 (2004).
[20] J. V. Sánchez-Pérez, D. Caballero, R. Mártinez-Sala, C. Rubio, J. Sánchez-Dehesa, F. Meseguer, J. Llinares, and F. Gálvez, Phys. Rev. Lett. **80**, 5325 (1998).
[21] Y. Y. Chen and Z. Ye, Phys. Rev. Lett. **87**, 184301 (2001).
[22] C. Goffaux, J. Sánchez-Dehesa, A. L. Yeyati, Ph. Lambin, A. Khelif, J. O. Vasseur, and B. Djafari-Rouhani, Phys. Rev. Lett. **88**, 225502 (2002).
[23] F. Cervera, L. Sanchis, J. V. Sánchez-Pérez, R. Martínez-Sala, C. Rubio, F. Meseguer, C. López, D. Caballero, and J. Sánchez-Dehesa, Phys. Rev. Lett. **88**, 023902 (2002).
[24] B. C. Gupta and Z. Ye, Phys. Rev. E **67**, 036603 (2003).
[25] J. B. Pendry, Phys. Rev. Lett. **85**, 3966 (2000).
[26] J. G. Berryman, J. Acoust. Soc. Am. **68**, 1809 (1980).
[27] J. Mei, Z. Liu, W. Wen, and P. Sheng, Phys. Rev. Lett. **96**, 024301 (2006).
[28] *FEMLAB Modeling Guide*, Version 3.1i (Comsol AB, Stockholm, 2004).
[29] S. D. Holland and D. E. Chimenti, Ultrasonics **42**, 957 (2004).